Proc. Natl. Acad. Sci. USA
Vol. 79, pp. 6151–6155, October 1982
Biochemistry

A bent monomeric conformation of myosin from smooth muscle

(myosin rod hinge/filament assembly/regulatory light chains)

KATHLEEN M. TRYBUS, TED W. HUIATT*, AND SUSAN LOWEY

Rosenstiel Basic Medical Sciences Research Center, Brandeis University, Waltham, Massachusetts 02254

Communicated by William P. Jencks, July 6, 1982

ABSTRACT **Smooth muscle myosin filaments formed in 0.15 M KCl are depolymerized by MgATP to a 10S component, rather than to the 6S component typical of myosin monomer in high salt concentrations. This 10S species is also monomeric as determined by sedimentation equilibrium and calculated from the diffusion and sedimentation coefficients. The conformation of 10S myosin is, however, very different from that of 6S myosin, which has a flexible but extended rod. The Stokes radius and the viscosity of 10S myosin are less than those of 6S myosin, consistent with a structure in which the rod is bent. Electron microscopy of rotary-shadowed preparations confirmed that the light meromyosin region of the rod is bent back on subfragment 2, that region of the rod adjacent to the two globular heads. MgATP and dephosphorylation of the 20,000 molecular weight light chain increase the amount of 10S myosin present in 0.15 M KCl; addition of salt converts 10S myosin back to the typical 6S conformation. We conclude that smooth muscle myosin preferentially forms a bent or folded conformation instead of the extended shape usually associated with skeletal muscle myosin, provided that the salt concentration is kept sufficiently low.**

The stability of smooth muscle myosin filaments in MgATP depends on the state of phosphorylation of the 20,000 molecular weight light chain (LC_{20}). Dephosphorylated gizzard myosin filaments are dissociated by approximately stoichiometric amounts of MgATP, whereas phosphorylated filaments remain largely assembled even in millimolar MgATP, as shown by turbidity measurements and electron microscopy (1, 2). Similar results were obtained with nonmuscle myosin filaments from thymus and platelets (3).

Dephosphorylated gizzard myosin filaments in 0.15 M KCl were completely depolymerized by MgATP to a 10S component (2). At higher salt concentrations, gizzard myosin sedimented at 6 S in the presence or absence of MgATP. Because the sedimentation coefficient of myosin in solutions with low salt concentrations was approximately twice that of monomer in high concentrations of salt, it was suggested that 10S myosin might be a dimer that was dissociated to monomer by high concentrations of salt (2). An antiparallel dimer has been proposed as an intermediate in the assembly of side-polar filaments, a structure unique to smooth muscle and nonmuscle cells (4–6).

Here we show that 10S myosin is not a dimer, but a monomer in which the rod is folded back upon itself such that the light meromyosin (LMM) region interacts with its own subfragment-2 (S-2) region. Addition of salt reforms the 6S conformation in which the rod is extended. The salt concentration thus has a large effect on the conformation of monomeric smooth muscle myosin, with this unusual bent form occurring at physiological ionic strength.

The publication costs of this article were defrayed in part by page charge payment. This article must therefore be hereby marked "*advertisement*" in accordance with 18 U. S. C. §1734 solely to indicate this fact.

MATERIALS AND METHODS

Preparation of Calf Aorta Myosin. Myosin was prepared as described by Megerman and Lowey (7). To minimize phosphorylation of myosin by light chain kinase, 1 mM EGTA was added to all buffers, and MgATP was added to the crude myosin just prior to gel filtration. In this way, myosin was isolated with <10% phosphorylation. Myosin concentration was determined from $A_{280}^{1\%} = 4.8$.

Gel Electrophoresis. $NaDodSO_4$/polyacrylamide gel electrophoresis was performed according to the method of Laemmli (8), with a 5–20% gradient of acrylamide and a 4% stacking gel. Crosslinked myosin was separated on 2.5% acrylamide/0.5% agarose slab gels in the Laemmli buffer system. Phosphorylated and dephosphorylated LC_{20}s were separated on glycerol/acrylamide gels. The running gel contained 40% (vol/vol) glycerol and 10% acrylamide; the stacking gel, 40% glycerol and 3.5% acrylamide. The running and gel buffers were 20 mM Tris/glycine, pH 8.6 (9). Myosin samples were applied to the gel in 30 mM Tris/glycine, pH 8.6/8 M urea/0.2 mM EDTA/0.1% 2-mercaptoethanol.

Crosslinking. A 20 mg/ml solution of dimethyl suberimidate was prepared immediately before use. Myosin at 1 mg/ml (10 mM KP_i, pH 7.5/5 mM $MgCl_2$/1 mM EGTA/1 mM MgATP/0.15 or 0.6 M KCl) was crosslinked by addition of dimethyl suberimidate at 6 mg/ml for 1 hr at room temperature. As determined by sedimentation velocity, crosslinked 10S myosin remained in the 10S form even in 0.6 M KCl.

Analytical Gel Filtration. A 1.6 × 90 cm column equipped with flow adaptors was packed with Sepharose 4B. Approximately 220 14-drop fractions were collected at a flow rate of 110 drops/hr. A calibration curve for the column was obtained by plotting the known Stokes radius of standard proteins versus $erf^{-1}(1 - K_d)$. K_d is defined as $(V_e - V_o)/(V_i - V_o)$, in which V_e is the elution volume of the protein samples, V_o is the excluded volume, and V_i is the included volume; erf^{-1} is the inverse error function that linearizes the relationship between Stokes radius and K_d (10).

Centrifugation. Sedimentation velocity experiments were carried out in a Beckman model E analytical ultracentrifuge at 20°C, using the absorption optical system for protein concentrations <1 mg/ml and the schlieren optical system for higher concentrations. Diffusion coefficients were determined in a 12-mm synthetic boundary cell by using interference optics. The distance between one-fourth and three-fourths of the total concentration (assuming 4 fringes per mg per ml of protein) was used as a measure of boundary width (11). In one case, schlieren optics and the height–area method were used to determine the diffusion coefficient. High-speed sedimentation equilibrium

Abbreviations: LMM and HMM, light and heavy meromyosin; S-1 and S-2, subfragment 1 and 2; LC_{20}, 20,000 molecular weight light chain.

* Present address: Muscle Biology Group, Iowa State University, Ames, IA 50011.

was performed at 5°C, using the six-channel, 12-mm equilibrium cell (12) in the AnE rotor operated at 8,000 rpm. Initial protein concentrations were 0.1, 0.3, and 1 mg/ml. Interference fringes were scanned on a flatbed densitometer (13), and point-by-point molecular weight averages were calculated by using the computer program of Roark and Yphantis (14).

Circular Dichroism. Spectra were recorded on a Cary spectropolarimeter with a circular dichroism attachment, using 0.5-mm cells and a protein concentration of 0.5 mg/ml. Percentage α-helix was calculated from the empirical relationship of Greenfield and Fasman (15).

Electron Microscopy. Electron microscopy was performed on a Philips EM 301 microscope operated at 80 kV. Myosin samples were rotary shadowed according to the method of Tyler and Branton (16).

RESULTS

Sedimentation Behavior of Myosin Monomer and Polymer. Smooth muscle myosin was purified from the calf aorta. A $NaDodSO_4$/polyacrylamide gel of the purified myosin showed no degradation of the heavy chain or the two light chains (Fig. 1*A*). The degree of phosphorylation of LC_{20} was determined by glycerol/acrylamide gel electrophoresis (Fig. 1*B*). Filaments were formed from dephosphorylated myosin by dialysis from 0.6 M KCl to 0.15 M KCl (10 mM KP_i, pH 7.5/5 mM $MgCl_2$/1 mM EGTA) over a period of 24 hr.

The sedimentation pattern of the dephosphorylated filaments is shown in Fig. 2 (upper patterns). As reported by Suzuki *et al.* (2), addition of 1 mM MgATP to dephosphorylated filaments depolymerized the polymer (Fig. 2, lower patterns). Even in the absence of MgATP, however, there is a considerable amount of the slow-moving boundary in equilibrium with polymer. The sedimentation coefficient of the slow-moving boundary is 10 S whether or not MgATP is present.

The 10S myosin is converted to the 6S species by the addition of KCl to 0.6 M (Fig. 3). The transition between the two states occurs between 0.2 and 0.3 M KCl in the presence or absence of MgATP, although MgATP shifts the transition to 6 S to slightly higher salt concentrations. The shapes of the 6S and 10S boundaries at identical concentrations are very different. The 6S boundary is hypersharp and diffuses very little, whereas the 10S boundary is broad and symmetrical and diffuses more rapidly. Because a 10S dimer would have a diffusion coefficient similar to that of a 6S monomer, the observed difference in diffusion suggested that the 10S component may not be a simple dimer. A determination of the molecular weight of the 10S component was undertaken to resolve this question.

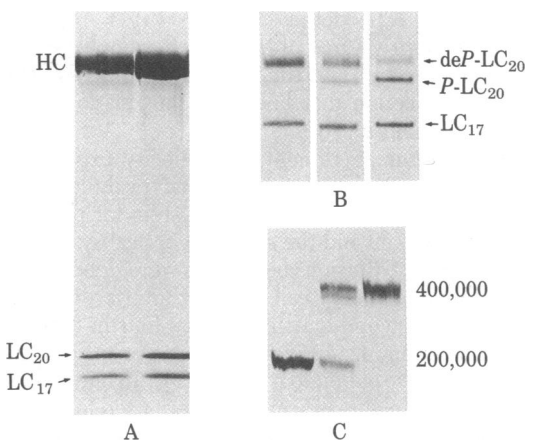

FIG. 1. (*A*) $NaDodSO_4$/polyacrylamide gel (5–20% gradient of acrylamide) of purified calf aorta myosin, showing the heavy chain (HC) and the 20,000 and 17,000 molecular weight light chains ($L2_{20}$, LC_{17}). (*B*) Separation of dephosphorylated (de*P*-LC_{20}) and phosphorylated (*P*-LC_{20}) LC_{20} on a glycerol/acrylamide gel. (*C*) $NaDodSO_4$/polyacrylamide gel of myosin crosslinked with dimethyl suberimidate.

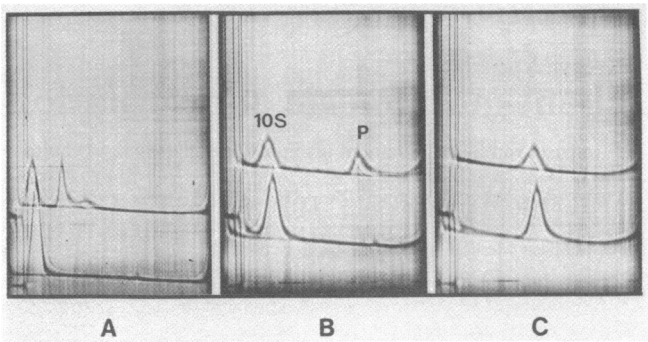

FIG. 2. Sedimentation pattern of dephosphorylated filaments in the absence (upper patterns) or presence (lower patterns) of 1 mM MgATP. In the absence of MgATP, two polymer peaks (47S and 76S) and a slow-moving boundary with a sedimentation coefficient of 10 S are observed at a protein concentration of 4 mg/ml. Addition of millimolar MgATP to the dephosphorylated filaments (lower patterns) depolymerized the polymer to the 10S component. (*A*) Patterns 32 min after reaching a rotor speed of 20,000 rpm. After 55 min, the rotor was accelerated to 60,000 rpm. (*B*) Patterns 2 min and (*C*) 24 min after reaching 60,000 rpm, bar angle 60°. Conditions: 10 mM KP_i, pH 7.5/0.15 M KCl/5 mM $MgCl_2$/1 mM EGTA/±1 mM MgATP, 20°C.

Molecular Weight of the 10S Component. Myosin in the 10S form was obtained by addition of 1 mM MgATP to dephosphorylated filaments in 0.15 M KCl. Any filaments that remained were pelleted in the preparative centrifuge. The molecular weight of the 10S component was first estimated from the sedimentation and diffusion coefficients extrapolated to zero concentration, $s^0_{20,w}$ and $D^0_{20,w}$ respectively. Figure 4*B* shows the diffusion coefficients of myosin in 0.6 M KCl and in 0.15 M KCl as a function of protein concentration. Although the value of $D^0_{20,w}$ as measured by boundary spreading is only approximate, nevertheless, the diffusion coefficient of 10S myosin is twice that of 6S myosin. The sedimentation coefficients are also plotted as a function of concentration for the two species (Fig. 4*A*). Myosin in high concentrations of salt has an $s^0_{20,w}$ of 6.0 S; myosin in 0.15 M KCl has an $s^0_{20,w}$ of 10.3 S. As is typical of asymmetric molecules, the observed sedimentation coefficient of myosin at high salt concentrations decreased at higher protein concentrations. The sedimentation coefficient of myosin in low salt did not show this behavior, suggesting that

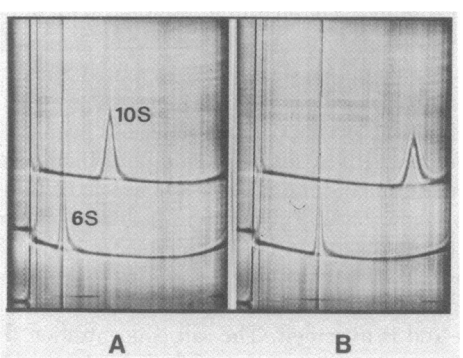

FIG. 3. Sedimentation pattern of myosin in 1 mM MgATP at 0.15 M KCl (upper patterns) or 0.6 M KCl (lower patterns). Dephosphorylated filaments were depolymerized by 1 mM MgATP to form 10S myosin (upper). Addition of 0.6 M KCl to 10S myosin (3 mg/ml) decreased the observed sedimentation coefficient to 4.5 S. Rotor speed, 60,000 rpm; bar angle, 60°. Patterns are shown 25 (*A*) and 57 (*B*) min after reaching speed. Conditions: 10 mM KP_i, pH 7.5/5 mM $MgCl_2$/1 mM EGTA/1 mM MgATP/0.15 or 0.6 M KCl, 20°C.

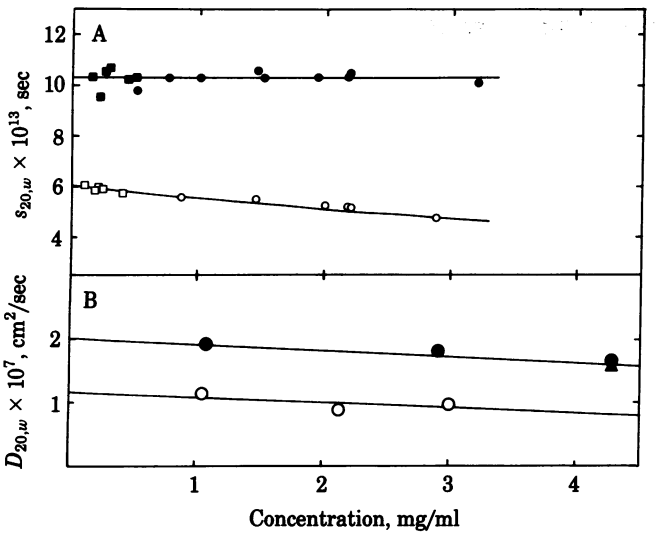

FIG. 4. Sedimentation and diffusion coefficients of myosin. (*A*) Dephosphorylated filaments in 0.15 M KCl were depolymerized by addition of 1 mM MgATP. The sedimentation coefficients of this component (filled symbols) and myosin in 0.6 M KCl (open symbols) are plotted as a function of concentration. The sedimentation coefficients were determined from schlieren patterns (circles) or by absorption optics (squares) at low protein concentration. The values of $s^0_{20,w}$ are 6.0 S in 0.6 M KCl and 10.3 S in 0.15 M KCl. (*B*) The diffusion coefficients of 10S myosin (filled symbols) and 6S myosin (○) are plotted as a function of concentration. ▲ indicates a value determined from schlieren patterns; all other values were determined by using interference optics. The values of $D^0_{20,w}$ are 1.1×10^{-7} cm²/sec in 0.6 M KCl and 2.0×10^{-7} cm²/sec in 0.15 M KCl. Rotor speed, 8,000 rpm. Conditions: 10 mM KP_i, pH 7.5/5 mM $MgCl_2$/1 mM EGTA/1 mM MgATP/0.15 or 0.6 M KCl, 20°C.

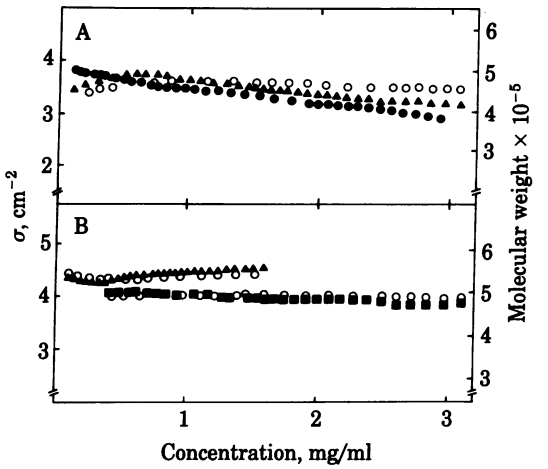

FIG. 5. High-speed sedimentation equilibrium of 6S and 10S myosin. The weight-average (filled symbols) and number-average (open symbols) molecular weights are plotted as a function of local cell concentration. $\sigma = M(1 - \bar{\nu}\rho)\omega^2/(RT)$. (*A*) The molecular weight of 6S myosin in 0.6 M KCl was determined directly after gel filtration (●) and after further concentration by precipitation with ammonium sulfate (▲). Initial loading concentration, 1 mg/ml. Molecular weight = $1.307 \times 10^5\ \sigma$. (*B*) Molecular weights of two different preparations of 10S myosin in 0.15 M KCl are plotted as a function of cell concentration. Initial loading concentrations, 1 mg/ml (■) and 0.3 mg/ml (▲). Molecular weight = $1.229 \times 10^5\ \sigma$. Conditions: 10 mM KP_i, pH 7.5/5 mM $MgCl_2$/1 mM EGTA/0.15 M KCl (1 mM MgATP) or 0.6 M KCl, 5°C. Rotor speed, 8,000 rpm.

10S myosin is less asymmetric than 6S myosin. There is also no evidence of dissociation of a 10S dimer into a 6S monomer, even at protein concentrations as low as 0.1 mg/ml.

The molecular weight of myosin in concentrated salt solutions calculated from $s^0_{20,w}$ and $D^0_{20,w}$ by the Svedberg equation is 527,000. Because both the sedimentation and diffusion coefficients of myosin in 0.15 M KCl are approximately twice those at high salt concentrations, the calculated molecular weight of 10S myosin is also that of a monomer, 470,000.

The molecular weights of the 6S and 10S species were measured directly by high-speed meniscus depletion sedimentation equilibrium. The weight-average and number-average molecular weights are plotted as a function of local cell concentration for 6S and 10S myosin in Fig. 5. The apparent molecular weight of myosin in 0.6 M KCl decreased at higher protein concentrations due to nonideality. The superposition of the values of the different weight averages at different initial loading concentrations (some data not shown) suggests that 6S myosin is a single homogeneous species with a molecular weight of 507,000. The molecular weights of two different preparations of 10S myosin are shown in Figure 5*B*. One preparation (▲) shows a small increase in the weight-average molecular weight above 1 mg/ml local cell concentration, but despite the indication of some higher molecular weight aggregates, 10S myosin is predominantly monomeric. This is shown more clearly by a second preparation (■), which gives a molecular weight of 500,000 at local cell concentrations up to 3 mg/ml. The sedimentation equilibrium data, therefore, unambiguously show that 10S myosin is monomeric.

Conformation of 10S Myosin. A myosin molecule with a sedimentation coefficient of 10S must have a very different conformation from that of the extended asymmetrical 6S myosin. Such a change in shape should be readily detected by gel filtration chromatography, a method that provides for the determination of the Stokes radius of a molecule. The elution volumes of proteins of known Stokes radius were determined in 0.15 M KCl and 0.6 M KCl (Fig. 6). Myosin was the only protein that changed its elution profile at the two ionic strengths. The 6S myosin in high concentrations of salt eluted with a K_d of 0.19, whereas 10S myosin eluted later with a K_d of 0.39. Myosin in high concentrations of salt has a calculated Stokes radius of 185 Å, which is consistent with the value determined from the cal-

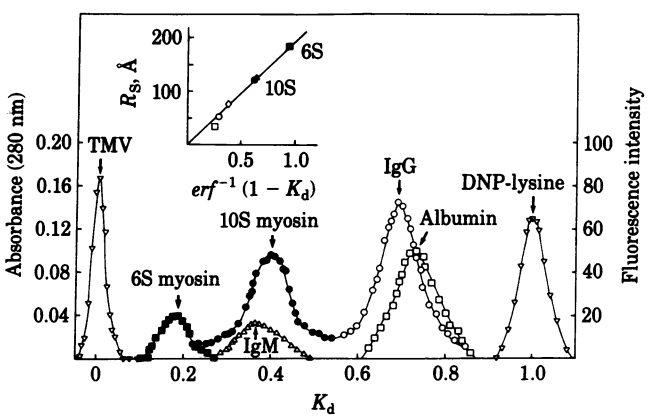

FIG. 6. Stokes radius of 6S and 10S myosin determined by gel filtration. The elution volumes of proteins of known Stokes radius—IgM (125 Å, △), skeletal muscle M protein (79 Å, ◇), IgG (53 Å, ○), and bovine serum albumin (37 Å, □)—were determined in 0.15 M and 0.6 M KCl. The K_d values of these proteins did not change with ionic strength. Void volume was determined with tobacco mosaic virus; included volume, with dinitrophenyllysine. Proteins in 0.15 M KCl/1 mM MgATP were detected by fluorescence; those in 0.6 M KCl were detected by absorbance at 280 nm or by fluorescence. (*Inset*) Calibration curve defined by the standard proteins. R_s, Stokes radius. The 6S myosin eluted with a K_d of 0.19; the 10S myosin eluted with a K_d of 0.39. This corresponds to Stokes radii of 185 Å for 6S myosin and 125 Å for 10S myosin. Conditions: 10 mM KP_i, pH 7.5/0.15 M KCl (1 mM MgATP) or 0.6 M KCl/5 mM $MgCl_2$/1 mM EGTA, 4°C.

ibration curve (Fig. 6 *Inset*), although asymmetric proteins can elute anomalously (17). The Stokes radius of 10S myosin determined from the calibration curve is 125 Å. This is also the calculated Stokes radius for heavy meromyosin (HMM), the two-headed subfragment of myosin that does not contain the LMM region of the rod. Because the hydrodynamic behavior of myosin is dominated by the rod (18), 10S myosin must have an effectively shorter rod than 6S myosin, such that its shape resembles that of HMM. Consistent with a more compact structure for 10S myosin, the intrinsic viscosity decreased from 2.5 dl/g in 0.6 M KCl to <1 dl/g in 0.15 M KCl. (Insufficient material precluded a more precise determination of this property.)

A decrease in α-helical content might be expected if the rod of 10S myosin is bent by a helix–coil transition. Circular dichroism measurements of 10S and 6S myosin showed no difference in secondary structure. A 10% or smaller change in helical content of the rod between the two species, however, would be difficult to detect.

Electron Microscopy of Rotary-Shadowed 10S Myosin. Although the hydrodynamic behavior of 10S myosin suggested that the rod was bent, it was clearly desirable to confirm this directly by rotary shadowing of single molecules. An electron micrograph of myosin at high salt concentration (Fig. 7*A*) shows long and extended tails with occasional bends as described by Elliott and Offer (19). In contrast, the apparent length of the rod of most 10S myosin molecules in the field (Fig. 7*B*) is shorter. The rod is bent such that the distal region of the rod (LMM) interacts with the region of the rod near the globular heads (S-2).

Because the bent form was not consistently observed by electron microscopy, the 10S conformation was stabilized by crosslinking with dimethyl suberimidate. The 200,000 molecular weight heavy chains of 6S and 10S myosin were crosslinked into a dimer (Fig. 1*C*), but only the 10S myosin was in the bent conformation as shown by electron micrographs of the crosslinked myosin molecules (Fig. 7 *C* and *D*). The heads are less distinct for both 6S and 10S myosin, presumably because they are crosslinked together. The results shown by these micrographs confirm and are consistent with all the hydrodynamic data.

DISCUSSION

Smooth muscle myosin from calf aorta has two different, stable, monomeric conformations. At high salt concentrations, 6S myosin is typically seen by electron microscopy as an asymmetric molecule with an extended rod region. The 10S conformation formed at 0.15 M KCl is a less asymmetric form in which the LMM region of the rod is bent back on the S-2; these two regions of the rod must interact closely because 10S myosin can be chemically crosslinked into the bent state. The two conformations are reversible, because 6S myosin dialyzed against low salt concentrations forms 10S myosin, and addition of salt reforms the 6S conformation. The amount of 10S myosin in equilibrium with filaments is increased when the LC_{20} is unphosphorylated and MgATP is present, although nucleotide is not essential for the 10S conformation in 0.15 M KCl.

The effect of the salt concentration on the conformation of the rod could be due either to a direct effect on the S-2/LMM junction or to an indirect effect mediated by the light chains.

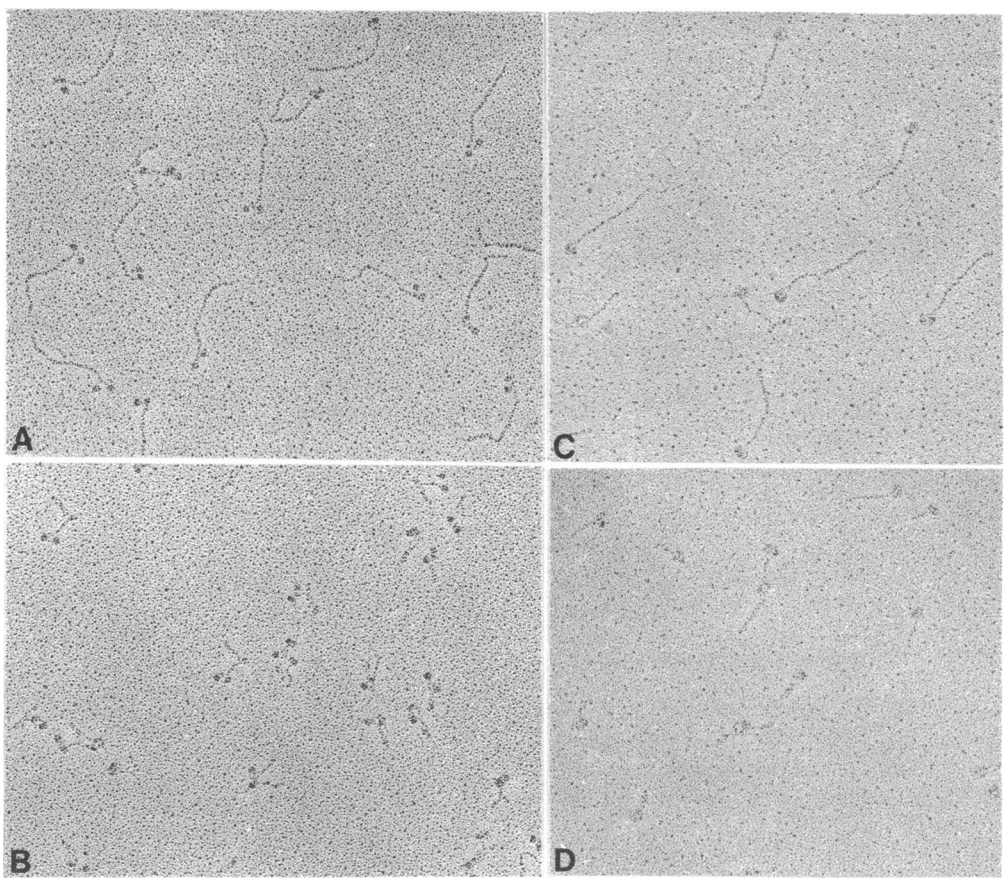

FIG. 7. Electron microscopy of rotary-shadowed 6S and 10S myosin. (*A*) The 6S myosin in 0.33 M ammonium acetate, pH 7.0. (*B*) The 10S myosin in 0.15 M KCl/3 mM KP_i, pH 7.5. (*C*) The 6S myosin crosslinked with dimethyl suberimidate, in 1 M ammonium acetate, pH 7.0. (*D*) The 10S myosin crosslinked with dimethyl suberimidate, in 1 M ammonium acetate, pH 7.0. In addition, all solutions contained 0.3 mM MgATP, 2 mM $MgCl_2$, 0.3 mM EGTA, and 66% (vol/vol) glycerol. (×76,500.)

Changes in the head region of myosin clearly can exert an effect on the rod because phosphorylation of the regulatory light chain or binding of MgATP to the head (3) alters filament stability. Salt-induced changes in the conformation of the alkali light chains of skeletal myosin (20) or the isolated dithionitrobenzoic acid light chain (21) have been detected by circular dichroism. The 20,000 molecular weight light chain of smooth muscle myosin may undergo similar changes in helical content with salt concentration. Although the location of the regulatory light chain of smooth muscle myosin in the head is not known, the homologous regulatory light chain from scallop myosin is believed to extend into the neck region near the subfragment-1 (S-1)/S-2 junction (22). In this position, changes in the regulatory light chain (phosphorylation, salt effects) could be transmitted to distal positions along the rod.

The bending observed in the smooth muscle myosin rod at low salt concentration occurred more frequently and at consistently greater angles than previously observed for skeletal myosin (19), although the solvent for skeletal myosin contained a high concentration of salt. A sharp bend in the rod of skeletal myosin occurred about 430 Å from the head/tail junction and provided indirect evidence for a hinge. A hinge has been postulated to account for contraction at constant sarcomere volume. The head (S-1) and S-2 regions of myosin could swing away from the filament backbone during contraction to allow S-1 to attach to actin at various interfilament distances (23). It has also been suggested that an α-helix-to-random-coil transition occurs in the hinge region of myosin to generate the actual tension produced during contraction (24). The bending observed in smooth muscle myosin does not seem to occur by any large helix–coil transition, because no change in circular dichroism was observed between 10S and 6S myosin.

Flexibility of the skeletal myosin rod has also been shown by analysis of rates of relaxation of electrical birefringence (25) and depolarized light scattering (26) and from observations of differential regions of thermal stability in the rod (27). From known dimensions of the head and rod, the translational and rotational diffusion coefficients and the intrinsic viscosity of myosin can be calculated. These calculated values do not agree with experimental values unless myosin is modeled with a flexible hinge at the S-2/LMM junction (18). The S-2/LMM junction is also a major site of attack by proteolytic enzymes (28), but there is no evidence that this susceptibility is due to a large non-α-helical region. The α-helical content of the rod is essentially the same as that of LMM and S-2 and the rod contains no proline residues (29). Amino acid analysis of the carboxyl region of long S-2 that is not common to short S-2 shows a slightly higher fraction of serine and glycine residues, which do not favor helix formation (30). Thus the region between S-2 and LMM may have a slightly different structure from the rest of the rod. It is not known whether smooth muscle myosin rod has a unique sequence that could account for the more flexible region observed.

These studies do not necessarily imply that dephosphorylated smooth muscle myosin *in vivo* is present as a bent monomer. Recent studies using rapid freezing techniques have clearly shown that dephosphorylated myosin in relaxed smooth muscle is filamentous (31). The flexibility observed in the dephosphorylated myosin monomer could be manifested in a more subtle way *in vivo*, such as in differences in myosin packing in the filament, which in turn could influence the interaction of myosin with actin. Filaments from relaxed and contracted smooth muscle may indeed be different, because early electron microscopy studies showed thick filaments only in contracted muscle (32), which led to the hypothesis that myosin in relaxed muscle was disassembled.

The most well studied of all myosins, namely skeletal muscle myosin, has not readily revealed this bent conformation. This does not imply that no bending occurs in skeletal muscle myosin (33), but it may be less pronounced than in smooth muscle myosin. Therefore, it is reasonable to suggest that this bent conformation may be directly related to some of the unusual physiological properties of smooth muscle myosin.

Note Added in Proof. Suzuki *et al.* (34) have recently concluded that 10S gizzard myosin is monomeric.

We thank Denise D. LeBlanc for assistance with the electron microscopy and John L. Woodhead for advice concerning the molecular weight calculations. This work was supported by grants from the National Institutes of Health (5 RO1 AM17350), the National Science Foundation (PCM 782 2710), and the Muscular Dystrophy Association to S.L. Work was done by K.T. during the tenure of a research fellowship from the American Heart Association, Northeast Massachusetts Division, no. 13-412-801. T.W.H. was the recipient of a National Research Service Award (5 F32 AM 06176-03) from the National Institutes of Health.

1. Onishi, H., Suzuki, H., Nakamura, K., Takahashi, K. & Watanabe, S. (1978) *J. Biochem. (Tokyo)* **83**, 835–847.
2. Suzuki, H., Onishi, H., Takahashi, K. & Watanabe, S. (1978) *J. Biochem. (Tokyo)* **84**, 1529–1542.
3. Scholey, J. M., Taylor, K. A. & Kendrick-Jones, J. (1980) *Nature (London)* **287**, 233–235.
4. Small, J. V. & Squire, J. M. (1972) *J. Mol. Biol.* **67**, 117–149.
5. Craig, R. & Megerman, J. (1977) *J. Cell Biol.* **75**, 990–996.
6. Hinssen, H., D'Haese, J., Small, J. V. & Sobieszek, A. (1978) *J. Ultrastruct. Res.* **64**, 282–302.
7. Megerman, J. & Lowey, S. (1981) *Biochemistry* **20**, 2099–2110.
8. Laemmli, U. K. (1970) *Nature (London)* **227**, 680–685.
9. Perrie, W. T. & Perry, S. V. (1970) *Biochem. J.* **119**, 31–38.
10. Ackers, G. K. (1967) *J. Biol. Chem.* **242**, 3237–3238.
11. Chervenka, C. H. (1973) *A Manual of Methods for the Analytical Ultracentrifuge* (Beckman Instruments, Spinco Division, Palo Alto, CA), pp. 83–86.
12. Ansevin, A. T., Roark, D. E. & Yphantis, D. A. (1970) *Anal. Biochem.* **34**, 237–261.
13. DeRosier, D. J., Munk, P. & Cox, D. J. (1972) *Anal. Biochem.* **50**, 139–153.
14. Roark, D. E. & Yphantis, D. A. (1969) *Ann. N.Y. Acad. Sci.* **164**, 245–278.
15. Greenfield, N. & Fasman, G. D. (1969) *Biochemistry* **8**, 4108–4116.
16. Tyler, J. M. & Branton, D. (1980) *J. Ultrastruct. Res.* **71**, 95–102.
17. Nozaki, Y., Schechter, N. M., Reynolds, J. A. & Tanford, C. (1976) *Biochemistry* **15**, 3884–3890.
18. García de la Torre, J. & Bloomfield, V. A. (1980) *Biochemistry* **19**, 5118–5123.
19. Elliott, A. & Offer, G. (1978) *J. Mol. Biol.* **123**, 505–519.
20. Mrakovčić-Zenic, A., Oriol-Audit, C. & Reisler, E. (1981) *Eur. J. Biochem.* **115**, 565–570.
21. Mrakovčić, A., Oda, S. & Reisler, E. (1979) *Biochemistry* **18**, 5960–5965.
22. Vibert, P. & Craig, R. (1982) *J. Mol. Biol.* **157**, 299–319.
23. Huxley, H. E. (1969) *Science* **164**, 1356–1366.
24. Harrington, W. F. (1971) *Proc. Natl. Acad. Sci. USA* **68**, 685–689.
25. Highsmith, S., Kretzschmar, K. M., O'Konski, C. T. & Morales, M. F. (1977) *Proc. Natl. Acad. Sci. USA* **74**, 4986–4990.
26. Highsmith, S., Wang, C., Zero, K., Pecora, R. & Jardetzky, O. (1982) *Biochemistry* **21**, 1192–1197.
27. Burke, M., Himmelfarb, S. & Harrington, W. F. (1973) *Biochemistry* **12**, 701–710.
28. Sutoh, K., Sutoh, K., Karr, T. & Harrington, W. F. (1978) *J. Mol. Biol.* **126**, 1–22.
29. Lowey, S., Slayter, H. S., Weeds, A. G. & Baker, H. (1969) *J. Mol. Biol.* **42**, 1–29.
30. Lu, R. C. (1980) *Proc. Natl. Acad. Sci. USA* **77**, 2010–2013.
31. Somlyo, A. V., Butler, T. M., Bond, M. & Somlyo, A. P. (1981) *Nature (London)* **294**, 567–569.
32. Kelly, R. E. & Rice, R. V. (1969) *J. Cell Biol.* **42**, 683–694.
33. Ueno, H. & Harrington, W. F. (1981) *Proc. Natl. Acad. Sci. USA* **78**, 6101–6105.
34. Suzuki, H., Kamata, T., Ohnishi, H. & Watanabe, S. (1982) *J. Biochem. (Tokyo)* **91**, 1699–1705.